Simulation of the Performance of Passenger Rail Vehicles under Blast Conditions in LS-DYNA®

Francois Lancelot, Ian Bruce, Devon Wilson, Kendra Jones
Arup
Przemyslaw Rakoczy
Transportation Technology Center Inc.

Abstract

The protection of the national transportation systems in the face of increasing terrorist threats is of critical importance. Arup North America Ltd (Arup) and Transportation Technology Center, Inc. (TTCI) have been contracted to conduct research to quantify the vulnerability of railcars and infrastructure to damage caused by the use of explosives. The main objectives of this ongoing research program is to develop tools to evaluate the performance of existing railcar structures, develop potential mitigation measures for current railcars, and investigate advanced security systems for future designs under blast conditions.
As part of this research work, Arup has developed detailed finite element (FE) models of a series of passenger railcars and investigated a number of different methodologies for applying blast loads in LS-DYNA. The methodologies investigated included pressure mapping onto the FE model, implementation of the ConWep equations, and a fully-coupled fluid structure interaction (FSI) approach using ALE formulation in LS-DYNA.
These techniques have been thoroughly validated against full scale blast tests carried out by TTCI and the most appropriate option for railcars blast performance evaluation has been determined.
This paper summarizes the modelling methodology, LS-DYNA analysis results and the outcomes of this joint Arup-TTCI investigation.

Keywords: *LOAD_BLAST_ENHANCED, FSI, ALE, Blast, Railcars

Introduction

TTCI and Arup are conducting a multiyear four-phase research program primarily directed at quantifying the vulnerability of passenger railcars to damage caused by explosives. An initial risk assessment identified four scenarios for the sizes and placements of explosive devices within railcars by terrorists [1]. These scenarios provided the bases of the investigations performed using LS-DYNA finite element (FE) blast models of representative railcars. The project focused on FE modeling and testing of three types of passenger railcars, light rail, transit, and commuter cars. The validated FE models are used to provide analytical means for predicting damage to the railcars and developing blast mitigation measures. This paper focuses on some of the material validation work, the tuning of analysis parameters, and provides comparison between analytical results and physical tests for the light rail car.

Overview of blast effect

When a high explosive substance is detonated, the resulting chemical reaction generates a large quantity of hot gases. These gases undergo a violent supersonic expansion that forces outwards and compresses the layer of surrounding air. This layer (the shock wave) contains most of the energy released and travels outwards from the center of the explosion. As the explosive charge is now fully used up, the total energy of the system is constant. Therefore, as the blast wave expands spherically outwards, the peak pressure at the blast front decreases.
The series of images in Figure 1 illustrates the blast wave as it propagates outward from the center of an explosion and dissipates.

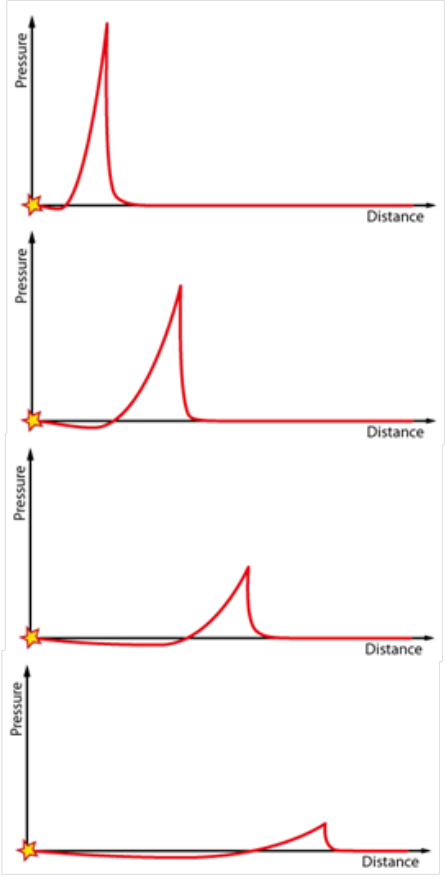

Figure 1 - Blast wave propagation - Pressure v. Distance from charge

When a blast wave impacts a solid surface, it is reflected off. The magnitude of the resulting pressure applied to the surface depends on the angle of incidence between the blast wave and the reflecting surface.

The detonation of high explosives inside a confined space produces two distinct phases. The first phase is from the propagation of the blast wave inside the structure and the resulting reflected waves. The second phase is the general increase of pressure inside the structure due to the gas generated by the explosion. Figure 2 shows a typical pressure versus time profile at a fixed point for a blast inside a confined space.

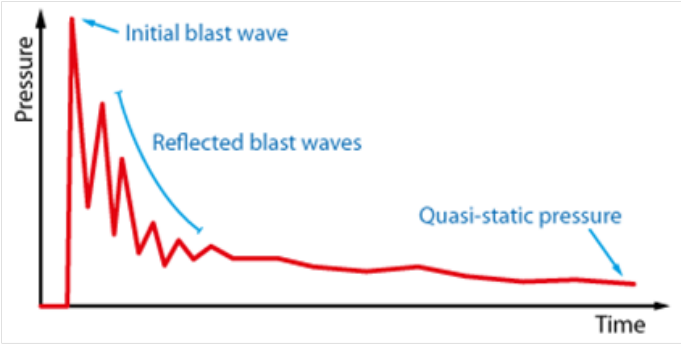

Figure 2 - Typical pressure v. time profile for a blast inside a structure

The final resulting pressure depends on the volume of the confined space, the quantity of gas generated by the explosion, and the amount of venting in the structure.

Railcar material characterization

Explosive loading produces very high strain rates in the surrounding structural materials. Structural steel and aluminum possess different stress-strain characteristics at high and low strain rates. To produce the most accurate blast predictions, stress-strain characterization tests were performed at different strain rates on material samples taken from the different railcar types tested.

Materials were selected for characterization based upon their prevalence in the car design as load bearing components. Tensile tests were performed on the specimens of the selected materials along the rolling direction (direction the material was rolled during manufacture) at strain rates of 0.0001s-1 and 0.1s-1, (representing low and medium strain rates) using an INSTRON® tensile tester, and 1,000 sec-1 (representing high strain rates) using a Hopkinson Bar Tension tester. Specimens prepared perpendicular to the rolling direction were also tested at a 1,000 sec-1 strain rate. Strain rates in the neighborhood of 1,000 sec-1 are experienced during blast loading of the test railcars [1].
Figures 3 and 4 show examples stress-strain results for the selected steel (COR-TEN) and aluminum (6351-T6 grade) materials. These plots compare averaged stress-strain results for all three strain rates considered. As expected, materials subjected to high strain rates exhibit also higher yield and ultimate strength [1].

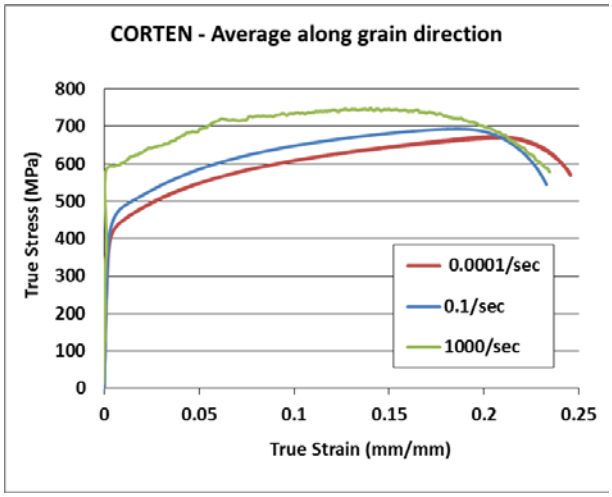

Figure 3 – COR-TEN steel - Averaged tensile results at different tested strain rates

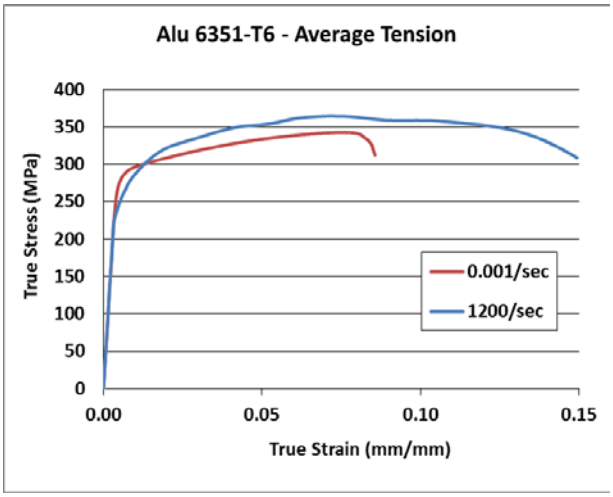

Figure 4 - Aluminum 6351-T6 - Averaged tensile results at different tested strain rates

Connection modelling and calibration of FE fixtures

In order to improve the overall modelling of the railcar structure, TTCI and Arup undertook to collect and test connection samples and to develop better-correlated connection models. New connection samples were fabricated and tested as well. These new samples enabled the assessment of additional joint connections where assembly coupons were difficult to collect from the tested railcars.

Arup constructed FE models to replicate each of the physical connection tests performed on the aluminum rivets and steel spot-welds. Modelling parameters for each connection were adjusted to achieve a better correlation to the physical test results.

TTCI tested a total of 36 connection samples taken from the test cars in areas unaffected by the test. New connection samples were fabricated using materials and manufacturing techniques similar to those used in the original rail car. Aluminum and steel samples were respectively riveted and spot welded. Test load conditions included: peel and shear for old samples, and peel, shear, multiple peel and tension for new samples. Examples of old aluminum riveted connections post testing are given in Figure 5 below.

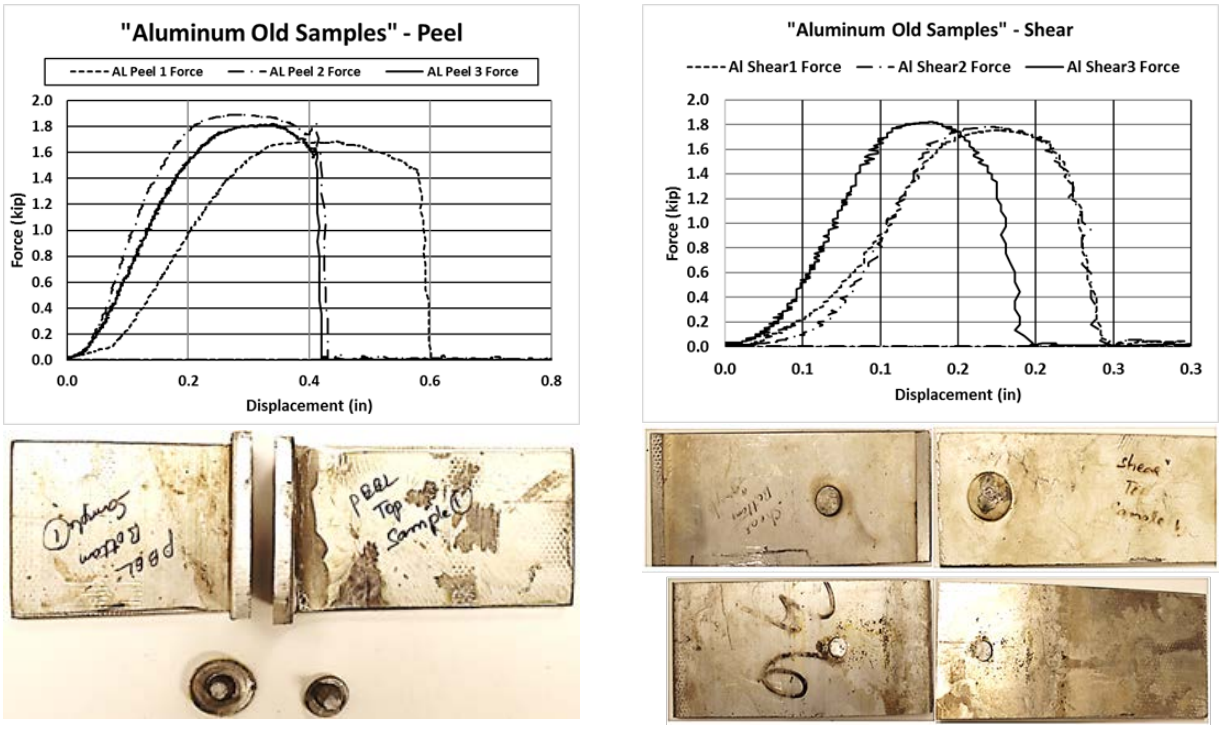

Peel test results **Shear test results.**

Figure 5 – 'Old' Aluminum riveted assemblies – Peel and lap-shear tests

FE Modeling

Rivets and spot welds were modeled with solid elements tied to the base material using tied surface-to-surface contacts. The spot-weld/rivet solids use *MAT_SPOTWELD_DAIMLERCHRYSLER in LS-DYNA [2]. This material model captures elastic-plastic material behavior with isotropic hardening and incorporates damage, or loss of material stiffness, as combined axial, shear and bending stresses approach a failure limit. The spot-weld elements are deleted once this failure, defined as ultimate strain, is reached.

Test assembly plates were modeled using shell elements with typical edge lengths between 5 mm and 15 mm (0.2 in and 0.6 in). For each of the load cases, the FE model reflected the test boundary conditions. Generic analysis model descriptions are given in Figure 6 below.

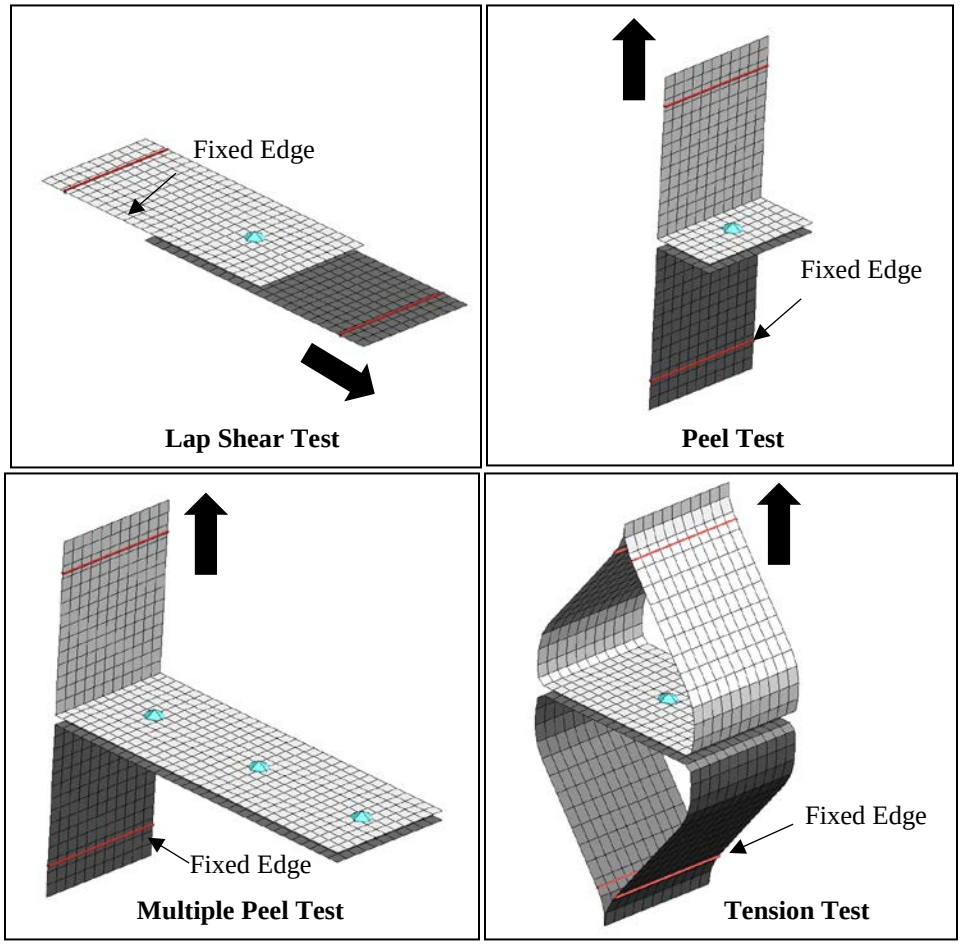

Figure 6 - Connection Tests- Simulation set ups

Load Application – Explicit solver

A prescribed ramped displacement was applied explicitly to the free edge of the models as illustrated in Figure 6. Results from the physical tests were used to define maximum displacement for each test case to ensure development of complete stress-strain curves up to failure. Force-displacement curves for each load case were compared to physical tensile test results.

Connection optimization - Results

The parameters of the connection models were iteratively modified to improve the correlation levels with experimental results. This optimization process was accomplished through modifying approximately 20 failure-related parameters in the spot-weld material model. Key parameters include normal, bending and shear strengths, along with values to capture combined loading effects, strain rate effects and the accumulation of damage, or strength reduction.

Results are presented below for some of the tests performed. Old and new samples exhibited different behavior during testing and were correlated with separate, independent models. Figures 7 and 8 below show reasonable correlation levels between experimental measurements and LS-DYNA simulation results on old rivet samples for the lap-shear and peel tests respectively.

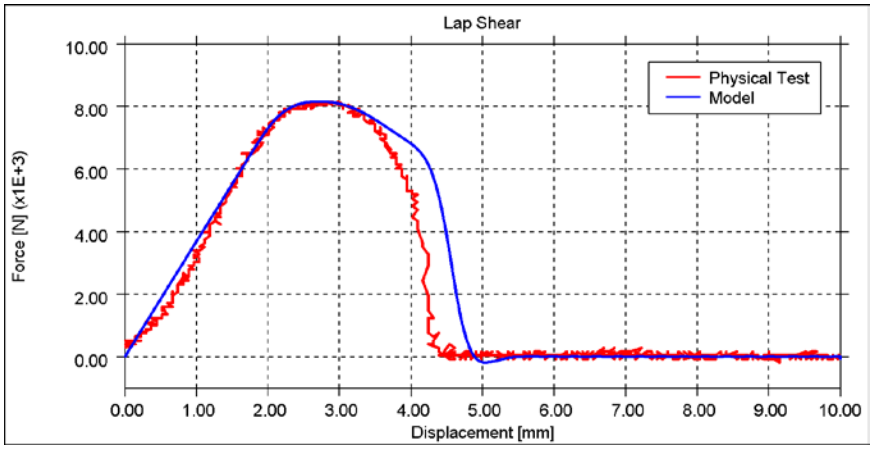

Figure 7 - Lap Shear force-displacement curve for old rivet sample

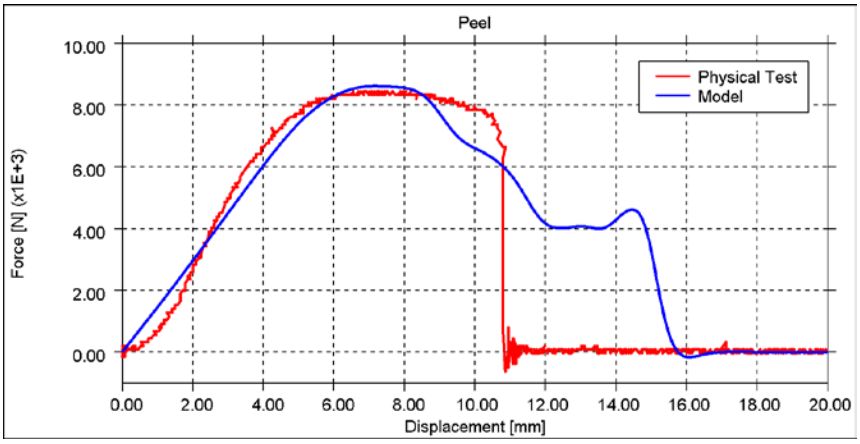

Figure 8 - Peel force-displacement curve for old rivet sample

Small scale blast testing and ALE parameter tuning

There are a number of different methodologies that can be used to apply the blast wave pressures onto a structure, each of which have their advantages and limitations. At the start of the study, three different techniques in LS-DYNA were investigated to determine the most appropriate for modeling a blast inside a passenger railcar:

1. The ConWep-based method using *LOAD_BLAST_ENHANCED capability. This function in LS-DYNA is based on the Kingery & Bulmash equations which are derived from empirical data. The relevant blast pressure loading on a given element is calculated at each timestep in the analysis based on the time since detonation, the distance from the charge center and the angle of incidence

2. An Air3d Computational Fluid Dynamics (CFD) analysis for pressure prediction followed by load mapping in LS-DYNA. Air3D is a CFD code developed by Cranfield University (UK) for modeling blast wave propagation. In this method, a standalone Air3D model is run first. The pressure time histories are extracted from this model for a large set of points on the railcar geometry. These pressure time histories are then mapped onto the LS-DYNA structural model

3. The LS-DYNA Arbitrary Lagrangian Eulerian (ALE) solver + Fluid Structure Interaction (FSI) using *CONSTRAINED_LAGRANGE_IN_SOLID. The ALE method takes the fluid mesh and performs a lagrangian step which deforms the mesh. Then an advection step is carried out to remap the distorted lagrangian mesh back on the original undeformed fluid (Eulerian) control volumes. This advection step can lead to the smoothing (dissipation) of rapid pressure changes (i.e. blast waves). The FSI method couples the fluid domain with the structural mesh. When a structural node is located in a fluid element a coupling force is applied to the node based on the fluid pressure. Conversely a pressure is also applied to the fluid to prevent it from flowing through the structure. A small scale study (detailed below) was carried out to determine the ALE/FSI parameters.

The full ALE+FSI approach requires specific numerical parameter settings. Testing and analysis of small sheet metal panels (referred to herein as Small Scale Tests) provided knowledge to calibrate the blast loading models in confined space conditions; it allowed the analysts to better characterize the response of sheet metal panels to blast loading and to enhance the accuracy of the FE models.
The complete railcar blast models assembled as part of this project are highly complex and contain thousands of elements. The small-scale study used a highly simplified test item comprising four panels fastened to cubic frames. Explosive charges at the geometric center of the frame applied blast pressures that forced the test panels outward. The simplified model and test items provided the opportunity to focus on the interaction between the blast loading and the response of the panels and to provide improved blast model characteristics for the complete railcar blast models.
Each test cube held two aluminum and two COR-TEN steel panels, as shown in Table 1. Four charge sizes and one to three tests of each charge size resulted in 9 physical tests in total.

Panel Name	Thickness
COR-TEN (Thick) – A 606	Gauge 14
COR-TEN (Thin) – A 606	Gauge 18
Al 1060-T6 (Thick)	4.8 mm (0.19 in.)
Al 1060-T6 (Thin)	4.1 mm (0.16 in.)

Table 1- Small scale tests – Panel details

FE Modeling

Figure 9 below shows the FE model of the frame structure. The blast source at the geometric center of the cube is also illustrated. Figure 10 describes the cube with its test panels, which are color-coded in accordance with the scheme used during physical testing.

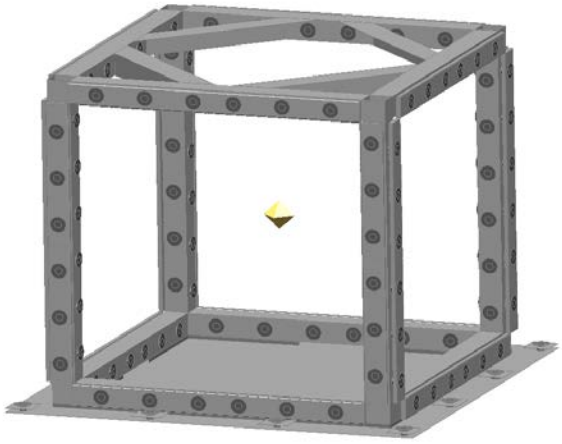

Figure 9 - Test cube analysis model – Frame structure

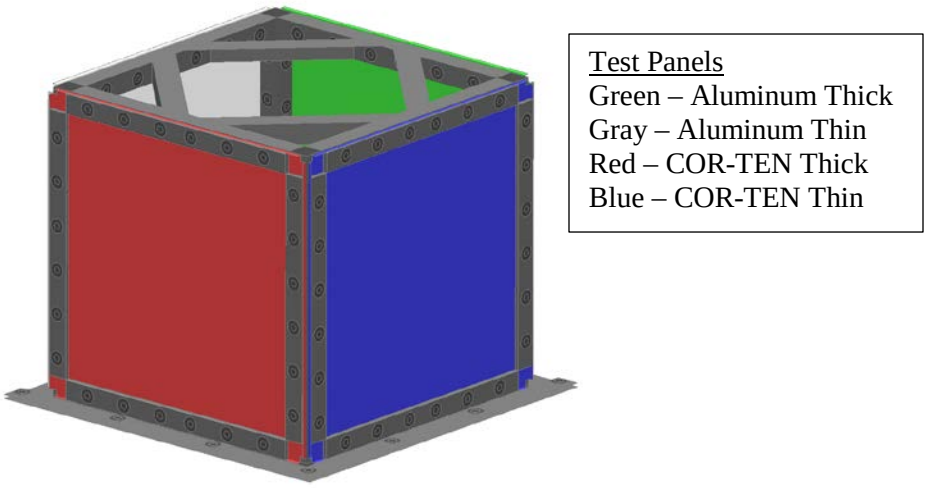

Figure 10 - Test cube analysis model – Panel details

The test cube panels and frame structure are modelled with shell elements (Type 2). Thick shell elements are used for the backing plates around the panel perimeter. These shell elements have a typical minimum edge lengths of approximately 5 mm (0.2 in). Bolt models primarily used 1D beam elements. Each beam element is approximately 12 mm (0.5in) in length. Null shells (tied back to the beam elements) representing the bolt shaft and head provided a contact surface and helped to capture local tearing in the test panels, as observed during physical tests. The air volume is meshed with solids having edge lengths of 50 mm (2 in). Figure 11 shows the

extent of the air volume around the cube. These element sizes were chosen to be of a similar size to those used in the full railcar models.

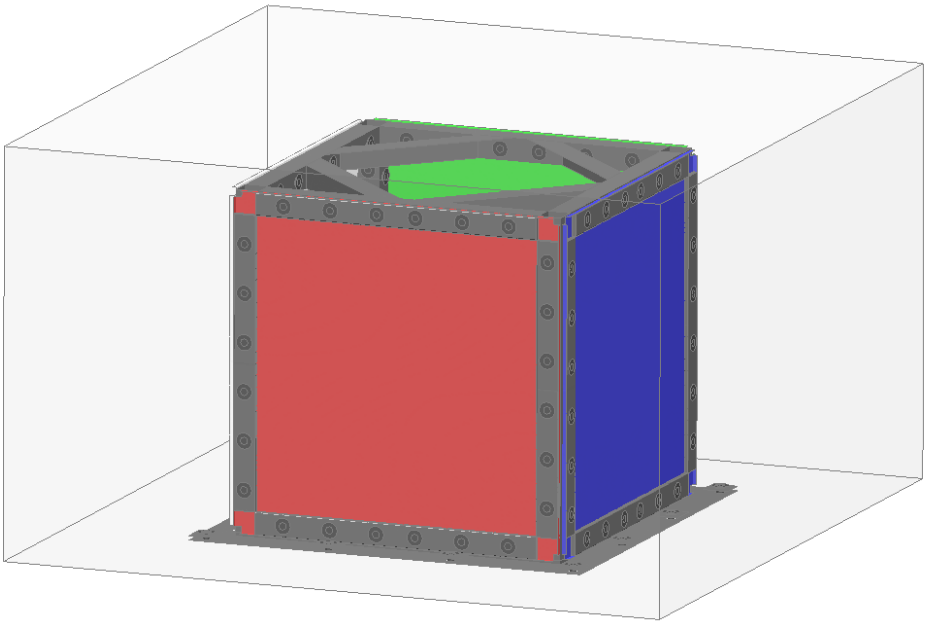

Figure 11 – Fluid control volume around test cube

Material Properties

The framing structure and bolt components used bilinear elastic-plastic material properties. American Society for Testing and Materials (ASTM) specifications were the source of material properties. Material models for COR-TEN and Aluminum panels calibrated from extensive physical tests and including nonlinear stress-strain data and strain-rate effects as described in the previous section were used in these analyses.

Connections and Component Interactions

Connections and interaction between the test cube components have been simulated as follows:

1. Surface contact: Frictional surface-to-surface contacts model the interface between test panels and both the frame and bolts
2. Tied contact: Tied node-to-surface contacts represent linear welds at the interface of the framing structure edge and base plate surface
3. Bolts are modeled explicitly as beam elements rigidly attached to the null shell elements representing the bold head/nut surfaces.

Boundary Conditions

A rigid plane was used to represent the ground. Atmospheric pressure is applied at the fluid volume boundaries.

Load Application

The blast source model is explicit and initiated according to the detonation velocity of the material. Full ALE/FSI method is applied to the small-scale blast simulations.

Results

A reasonably strong correlation of the panel maximum outward displacements has been achieved between physical tests and simulation results. It required tuning ALE control and constraint parameters in LS-DYNA.

Figures 12 shows respectively COR-TEN and Aluminum test panel deflections vs. time for a particular charge size. Test data appear with the test number designation "T#". LS-DYNA predictions are represented as solid lines. Test and analysis displacements agree fairly well, particularly for the deflection time-histories of aluminum panels. The COR-TEN Thin panel results show poorer agreement compared to all other panels. During testing, these panels consistently experienced the greatest displacements and the greatest occurrence of material failure (pull out around the bolts). Despite our efforts, the material model under-represents the failure, resulting in lower deflections in the model than recorded during tests. Nevertheless, overall, predicted displacement magnitudes remain in fairly good agreement with test data.

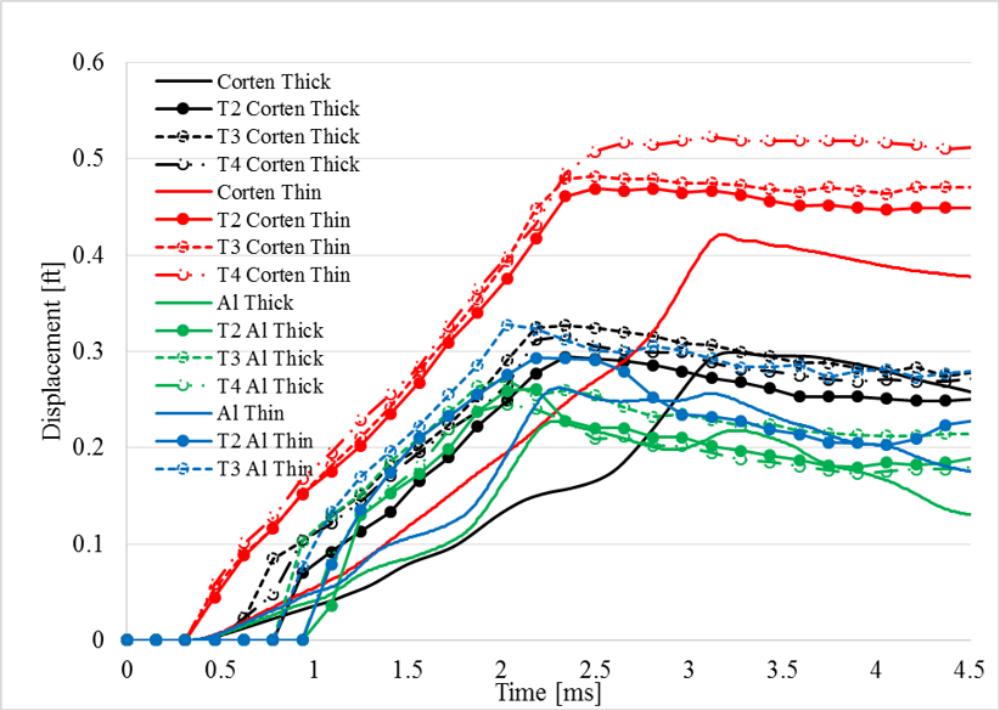

Figure 12 – Small scale testing – Panel displacements – Test results and simulation predictions

Small scale tests of aluminum and steel panel behavior under blast loads provided data for the analysis team to adjust parameters of the FSI model. This allowed to enhance the fidelity of the full railcar models and improve the accuracy of the LS-DYNA predictions.

Full Railcar Modelling in LS-DYNA

Arup constructed finite element models of the railcars. The models were developed from engineering drawings and measurements taken from the actual vehicles. The know-how and improved techniques resulting from the material, connection characterization and small scale testing phases were implemented in the full railcar model and used to select the most appropriate methodology for simulating the blast load to the carbody structures.

Light Rail Car Model

The model of light rail car is illustrated below. It includes the entire car structure with contacts and connections explicitly represented. Modeled interior components include the flooring, seats, partitions, and stanchions. Figure 13 shows the car structure and Figure 14 illustrates the interior of the model.

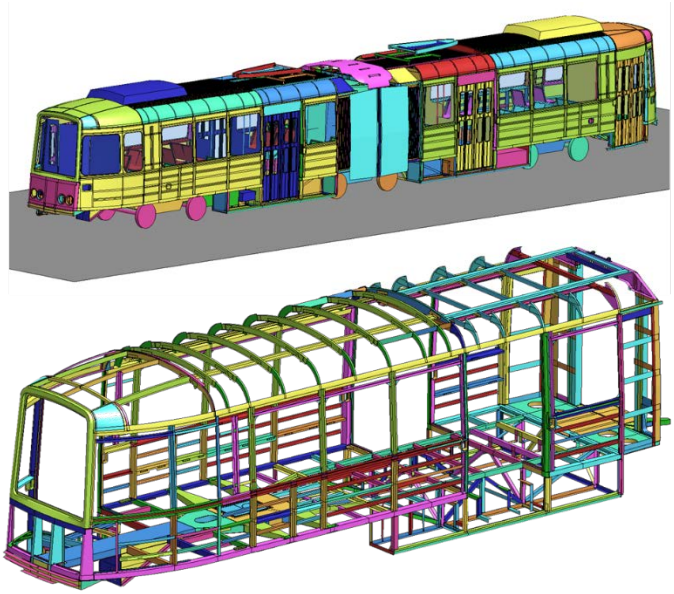

Figure 13 - Model of the light rail car structure

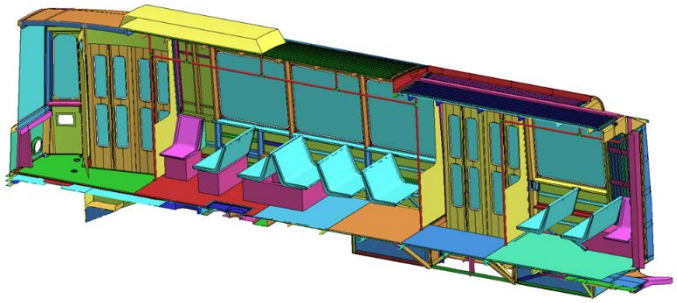

Figure 14 - Model of the light rail car interior

Blast tests vs Analysis results

Blast test – Internal charge

Test cars were articulated light railcars comprising two carbodies riding on three trucks.

All windows were blown out of both ends of the car by the charge that was placed in the north carbody. The air conditioner heat exchanger unit mounted on the roof of this carbody hit the catenary cable and kinked it, but did not sever it. The south end of the car experienced very little damage, but there were some loose debris inside the carbody. Peak-to-peak carbody motions were less than 10 mm (0.4 in). The car was pulled away from the test site by a locomotive after the test without difficulty. Seats across the aisle from the charge remained intact and attached. Only a modest amount of debris was present, due in part to removal of ceiling materials and ductwork as part of pretest asbestos abatement. Part of the blast vented through the car roof. Figures 15 and 16 show the exterior and the interior of the car after the test [1].

Figure 15 - Exterior of the light rail car after internal charge test

Figure 16 - Interior of the light rail car after internal charge test

The highest speed debris left the carbody at about 680 km/h (420 mph). Clusters of windows left the carbody at about 183 km/h (114 mph). All debris fell within a 73-m (240-ft) radius from the charge [1].

Full Vehicle Blast - Analysis results and comparison to test

Comparison of the three modeling methods showed the FSI model to be superior to the other methods. As shown in Figure18, the red and blue regions of wall skin separated from the structural framing in the FEM model, which compares favorably to the test image. Additionally, for parts of the car further from the blast, the FSI model correctly captures the appropriate magnitude of damage, i.e., the splitting of the roof.

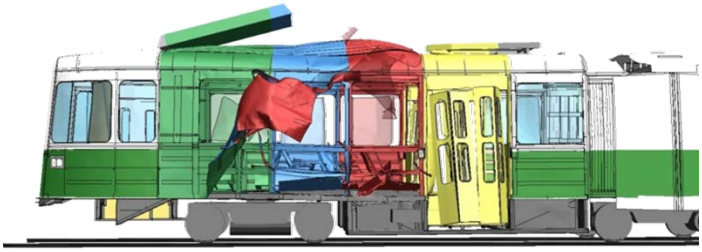

ConWep - *LOAD-BLAST

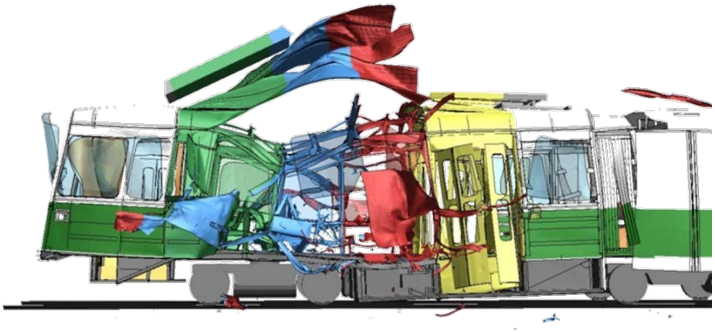

Mapped Air3D pressures

ALE-FSI Method

Physical test

Figure 18 - Damage level for different analysis methods - Light rail car model – Internal charge

Because of element size limitations and the postprocessing methods, the FSI model pressure curves are attenuated and flattened out. The pressure in these models is obtained by reading the pressure value within a given 100 mm (3.9 in) cube volume FSI element that envelopes the sensor location. The pressure is constant (averaged) over the entire FSI element. This leads to inherently flatter and smoother curves compared to the test data. The peak pressure value predicted by the FSI model cannot match the sharp peaks in the test data. However, a more important aspect for a structural analysis is the overall impulse that the pressure applies to the structure. A qualitative comparison of the curves indicates that the impulses match reasonably well. Figure 19 shows example pressure curve comparison between model and the test. The FSI analysis results match the test data quite well, and the limitations of the ConWep model for this situation are clear.

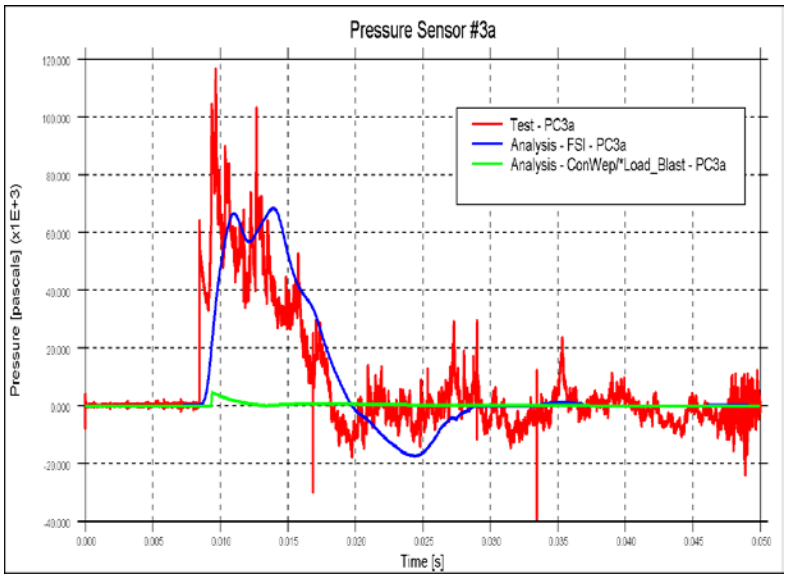

Figure 19 - Pressure comparisons for the Light Rail Car – Test v. ConWep v. FSI

This investigation confirmed that the ALE/FSI method in LS-DYNA is the most appropriate for our study given our scope, time and budget (despite also being the most computationally expensive). The ALE/FSI approach was used for all subsequent full car blast analyses.

More comparisons between test pressure measurements and FSI simulation results are provided in Figures 20 and 21.

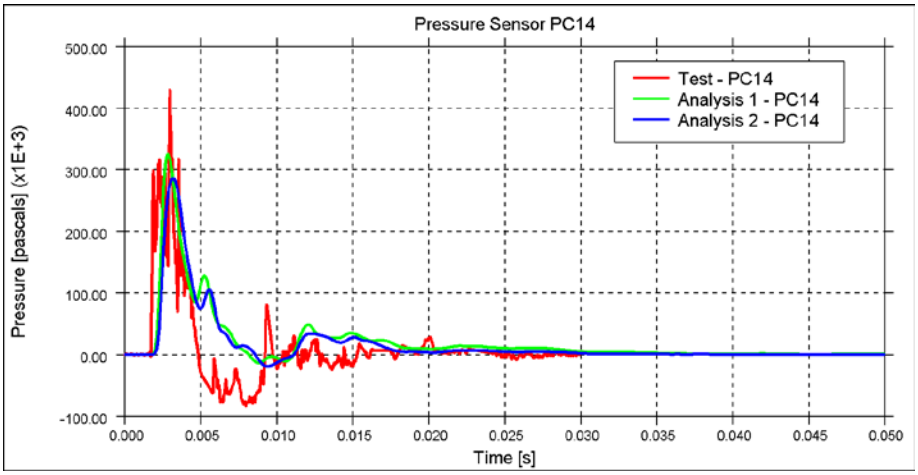

Figure 20 - Pressure comparison for Sensor PC14 – Test v. FSI analysis

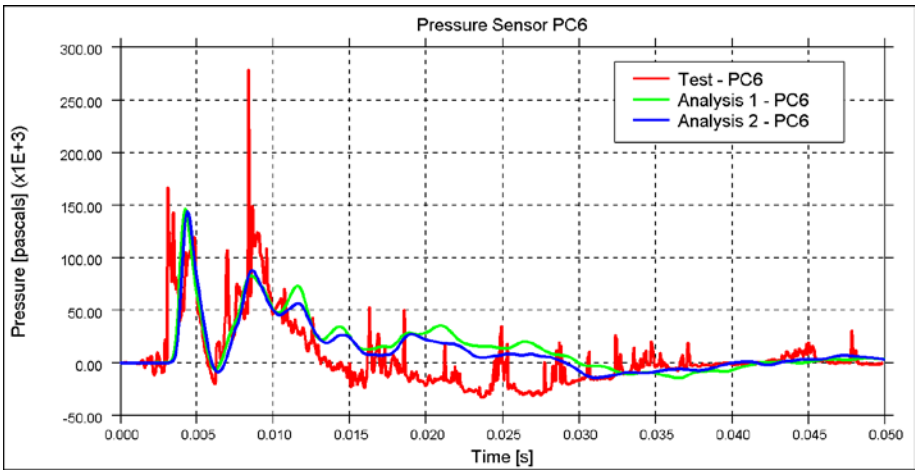

Figure 21 - Pressure comparison for Sensor PC6 – test v. FSI analysis

Conclusions

The experimental and computational work presented in this paper shows the approach followed by TTCI and Arup to quantify the vulnerability of railcars to explosive threats and lays a foundation for development of blast mitigation measures.

Various physical testing phases have been carried out to support the FE method validation: railcar material characterization, critical connection modelling optimization and small-scale blast for ALE tuning.

Although further refinement of the models is important and pressure prediction in particular remains imperfect, the FE models provide qualitative assessments of structural damage and prove capable of preliminary evaluation of countermeasures that may help to save lives and reduce injuries in the event of terrorist attacks on railcars using explosives. The work also provides experimental quantification of blast vulnerability of the tested cars that stands irrespective of the modeling work.

References

[1] – "Performance of Passenger Rail Vehicles Under Blast Conditions: Testing and Modeling", Przemyslaw Rakoczy, Nicholas Wilson, Ian Bruce and Stephanie Myers, 2017 Joint Rail Conference Philadelphia, Pennsylvania, USA, April 4–7, 2017, ISBN: 978-0-7918-5071-8

[2] - LS-DYNA Keyword User's Manual, Version 971. Livermore Software Technology Corporation (LSTC): Livermore, CA 94551-5110, USA, May 2007